Paper No.
10093

NACE INTERNATIONAL CORROSION 2010 CONFERENCE & EXPO

PROGRESS IN THE PREDICTION OF TOP OF THE LINE CORROSION AND CHALLENGES TO PREDICT CORROSION RATES MEASURED IN GAS PIPELINES

Yves GUNALTUN
Total S.A seconded at PTTEP. Shinawatra Tower III
1010 Vibhavadi - Rangsit Road. Chatuchak, Bangkok 10900 / Thailand

Ussama KAEWPRADAP, Marc SINGER, Srdjan NESIC
Institute for Corrosion and Multiphase Technology. Ohio University Research Park
342 West State Street. Athens, Ohio 45701 /USA

Suchada PUNPRUK, Matina THAMMACHART,
PTTEP/OPS/OMI. Shinawatra Tower III
1010 Vibhavadi - Rangsit Road. Chatuchak, Bangkok 10900 / Thailand

ABSTRACT

Bongkot is an offshore gas field in the Gulf of Thailand in operation since 1992. The sealines have been subjected to top of line corrosion (TLC) since the production start-up. After detection of the first TLC case in this field in 1999, different possibilities were investigated and implemented to reduce the corrosion rate to a reasonable value. Recently few leaks were experienced at cold spots like bare metal surfaces around subsea flanges or anode pads welding. It was clear that stabilisation does not take place at cold spots. TLC prediction for the sealines of different gas fields was necessary for prediction of leaks at such locations. The TOPCORP model was selected for this purpose. As a first step, the capabilities of this model were evaluated using data available from Bongkot field. This paper gives a short review of different prediction models, summarises selected model's main features, compares the predicted water condensation and corrosion rates to inspection results and discusses the capabilities of the model.

Key words: top of line corrosion, corrosion prediction, CO_2 corrosion, modeling

INTRODUCTION

About Bongkot Field and TLC Problems

Bongkot is an offshore gas field in the Gulf of Thailand (Figure 1) in operation since 1992. The first TLC case was detected in Bongkot sealines in 1999. Chemical treatments were immediately initiated. Chemical treatment efficiency was gradually improved by using better chemicals and tools by 2003 – 2004 following the progress achieved in research and development projects. Inspections, using MFL type tools, showed important thickness losses up to 74 % along the first 1 to 5 km of sealines as a result of TLC. A UT tool was also used for the inspection of a few pipelines and it showed only 10 – 20 % thickness losses. Further investigations showed that the UT tool was not able to measure the remaining thicknesses accurately due to presence of corrosion products that had accumulated inside the localized corrosion features. It is very likely that these thick corrosion products also prevent the corrosion inhibitor (applied by TLCC –PIG, also called spray pig) to be effective.

Three leaks were experienced in two of the pipelines in 2008. The first leak was close to a sub sea flange connecting the inlet riser to the dogleg, where there was no pipe coating. Two other leaks occurred on another line at anode pads where the original pipe coating had been replaced by a thin epoxy layer after anode installation. Failure analysis confirmed that the failures were not the result of any parameter related the metallurgy of the pipe, flange or welding. The main cause identified was localized TLC. In these three cases the corrosion occurred on small pipe surfaces where the water condensation rates were high when compared with other pipe surface locations (cold spot corrosion[1]).

In order to evaluate the risk of leaks for each sealine it was necessary to predict the corrosivity (mainly water condensation rate and corrosion rate) in all pipelines, especially at cold spots. For this purpose it was decided to first determine the capabilities of the selected model for such prediction. The purpose of the present study is not so much to validate the software, but more to identify areas where the predictions are significantly inaccurate (over or under predictions) and then attempt to explain the reasons why they occurred. It is hoped that this effort will facilitate further improvement of the model.

About Prediction of Top of the Line Corrosion

History of TLC prediction

In the past twenty years, TLC has been the subject of intensive research. DeWaard[2] proposed the first modeling approach to TLC based on his famous full pipe flow empirical equation. DeWaard introduced a correcting factor F_{cond}=0.1 in order to adapt his model to condensing conditions for condensation rates below an experimentally determined critical rate of 0.25 mL/m^2/s. The correlation proposed by DeWaard[2] (1) gives an extremely conservative prediction. It is detailed below:

$$CR = F_{Cond} \times 10^{\left(5.8 - \frac{1710}{T_K} + 0.67 \times \log(p_{CO2})\right)} \quad (1)$$

With pCO_2: Partial pressure of CO_2 (bar)
T_k: Temperature (K)
F_{cond}: 0.1
CR: Corrosion rate (mm/year)

In 2000, a new model was proposed by Pots et al[3] and it took into account the competition between the scale formation rate as compared to both the iron dissolution and the condensation rate. This so

called “Super saturation model” is based on the calculation of the concentration of iron at saturation under film forming conditions. The corrosion rate, calculated using the formula below (2), is equated with the precipitation rate (3), and calculated using an equation developed by Van Hunnik[4]. The concentration of Fe^{2+} which is present on both sides of the equation is calculated and re-injected into the corrosion rate equation.

$$CR = \frac{M_{Fe} \times 10^6 \times 24 \times 3600 \times 365}{\rho_{Carbonsteel}} \times \left[Fe^{2+}\right]_{\sup ersat} \times \frac{WCR}{\rho_w} \quad (2)$$

With CR: Corrosion rate (mm/y)
WCR: Water condensation rate (g/m^2/s)
ρ_w: Water density (g/m^3)
[Fe^{2+}]: Iron concentration (mol/l)
M_{Fe}: Iron molecular weight (55.847 g/mol)
$\rho_{carbonsteel}$: Density of a typical carbon steel (7860000 g/m^3)

$$PR = A_p \times e^{\frac{-E_a}{RT}} \times K_{sp} \times (s-1)(1-\frac{1}{s}) \text{ and } s = \frac{\left[Fe^{2+}\right] \times \left[CO_3^{2-}\right]}{Ksp} \quad (3)$$

With PR: Precipitation rate converted in mm/year
A_p: Constant
Ea: Activation energy (KJ/mol)
R: Ideal gas law (J/K/mol)
T: Temperature (K)
s: $FeCO_3$ saturation
Ksp: $FeCO_3$ solubility product (mol^2/l^2)

A complete chemistry analysis including the electro-neutrality equation, the dissociation equations and the CO_2 solubility need to be implemented as well. Pots et al[3] insisted on the importance of correctly evaluating the condensation rate in order to accurately predict the corrosion rate. However, no clear guidelines on how to calculate it were provided.

In 2002, Vitse[5-7] completed a thorough experimental and theoretical study on the TLC caused by carbon dioxide. Vitse developed a mechanistic film-wise condensation model based on the Nusselt theory and a semi-empirical corrosion model adapted to TLC scenario. The condensation model is based on the assumption that a continuous film of liquid covers the steel surface at the top of the line (film-wise condensation). Vitse acknowledges that while this approach is valid to estimate the condensation rate on the side of the pipe, it is not ideal to cover the condensation process happening at the top (11 to 1 O’clock position) which is drop-wise[8]. Nevertheless, the corrosion model constituted a considerable breakthrough in the understanding of the mechanisms involved in TLC. Once the value of the condensation rate was obtained, Vitse proposed to conduct a Fe^{2+} flux balance on a control volume, taking into account the fluxes of Fe^{2+} created by corrosion, removed by $FeCO_3$ precipitation and transported by condensed water film convection. A schematic representation of this approach is presented in FIGURE 2. The corrosion calculations are based on the electrochemical model developed by Nesic in 1996[9] which was modified in order to include the influence of corrosion product film on the corrosion rate once the saturation in $FeCO_3$ is reached. It was done by introducing an empirical correcting factor K which would represent the covering effect of the $FeCO_3$ film underneath which no corrosion would occur. This factor was defined experimentally but was correlated with the scaling tendency (ratio of corrosion and precipitation rate) (4).

$$\frac{d\left[Fe^{2+}\right]}{dt} = \frac{1}{\delta} \times \left[K \times CR - (1-K) \times PR - WCR \times \left[Fe^{2+}\right]\right] \quad (4)$$

With Fe^{2+}: Concentration of iron ion (mol/m^3)
T: Time (s)
CR: Corrosion rate (mol/m^3/s)
PR: Precipitation rate (mol/m^3/s)
WCR: Water condensation rate (m^3/m^2/s)
δ: Liquid film thickness (m)
K: Covering factor

Vitse's method gave insight as to how to model TLC phenomena and it constituted a considerable improvement in the understanding of TLC without being a fully mechanistic corrosion model.

In 2007, Nyborg[10] developed a new empirical equation for TLC prediction through experimental work. It is based on the concept that TLC is limited by the amount of iron which can be dissolved in the thin film of water condensing. According to Nyborg, the TLC rate can be modelled as proportional to the water condensation rate, the iron carbonate solubility and a supersaturation factor. The empirical equation (5) is displayed below and is valid only for low acetic acid content (<1 mM), low to medium carbon dioxide partial pressure (<3 bars) and no presence of H_2S:

$$CR = 0.004 \times WCR \times C_{Fe^{2+}} \times (12.5 - 0.09 \times T) \quad (5)$$

With CR: Corrosion rate (mm/y)
WCR: Water condensation rate (g/m^2/s),
C_{Fe2+}: Solubility of iron ions (ppm_w)
T: Temperature (°C)

Nyborg noted that the solubility of iron ion was a function of temperature, total pressure, CO_2 partial pressure and glycol concentration and was calculated with an in-house pH and solubility program. Although no detail was provided on how the condensation rate was calculated, Nyborg stated that the importance of predicting an accurate condensation rate as it would have a much more pronounced effect on TLC than, for example, the CO_2 partial pressure.

The same year, Zhang[11] presented the first fully mechanistic model for TLC prediction. The approach took into account the most important parameters in CO_2 TLC: condensation rate, gas temperature, CO_2 partial pressure and acetic acid concentration. Zhang model was selected for the present study and is described in greater detail in the following section.

In 2009, Remita[12] also extended the work proposed by Vitse[5] and developed a model for CO_2 corrosion under a thin liquid film. It followed a mechanistic approach for the chemical and electrochemical side of the phenomena but assumed a homogeneous composition within the film. Like Vitse, Remita introduced a covering factor θ in order to take into account the effect of $FeCO_3$ film formation, this factor being difficult to obtain.

In spite of the fact that a lot of progress has been made over the years on the understanding of the TLC mechanisms, none of the models so far proposed tackled the occurrence and prediction of localized corrosion. The first experimental study that was focused on this aspect and linked to the TLC phenomena was published by Amri[13], in an effort to relate pit growth and environmental conditions. However, no model has yet been proposed on this topic.

TLC prediction software selected in this study

Apart from the equations developed DeWaard[2], the models described above are not easily reproducible if the user does not have access to the original software. DeWaard's model, although quite simple, is also known to be very conservative.

The software used in the present study (Zhang's model[11]) was developed at a research institute in the USA(1) as part of joint industry project (JIP) that was focused on TLC and launched in 2000. The author's company is an active member of this JIP and has consequently access to the software which was selected for this study(2). The model covers the three main processes involved in Top of the Line Corrosion phenomena: dropwise condensation, chemistry in the condensed water and corrosion on the steel surface. As the condensation approach is drop-wise, the model is valid only for the 11-1 O'clock position in a pipe line. The condensation model is based on the heat and mass transfer theory and the chemistry in the condensed liquid is established through standard chemical and thermodynamic equations[14] The corrosion model is adapted from the mechanistic CO_2 corrosion approach developed terms of a four-stage scenario: nucleation, growth, coalescence and removal. An excellent review d by Nordsveen[15] and Nesic[16,17]. Zhang stated that from a statistical point of view every point on the metal surface has the same probability of being covered by liquid droplets and consequently assumed that the corrosion was uniform of the entire surface. It simplifies the mathematical approach from a three- dimensional situation (semi-hemispherical droplet) to a one-dimensional situation (liquid layer) as shown in FIGURE 3. The corrosion module includes chemical reactions (dissociation, dissolution and precipitation), transport of species to and away from the metal surface and the electrochemical reactions on the metal surface. Droplet growth is simulated by an increase in the liquid film with time until it reaches a calculated maximum size where the droplet disappears (falls or slides).

It is not the purpose of the present paper to describe the selected model in details and the reader is invited to refer to the original publication[11]. Nevertheless the equations governing the main aspects of the condensation and corrosion approach are presented below:

The condensation model is based on the phenomenon of dropwise condensation which has been studied extensively over the past sixty years. It can be described in paper summarizing the early findings in terms of mechanism and modeling was published by Rose[18] in 2002. As dropwise condensation is a random process, the common approach is to calculate the heat flux through a single droplet and to integrate the expression over an average distribution of drop sizes (6):

$$Q = \int_{r_{\min}}^{r_{\max}} q(r)N(r)dr \qquad (6)$$

With: Q: Total heat flux (W/m^2)
q(r): Heat flux through an individual droplet of radius r (W/m^2)
N(r)dr: Number of drops per area with radius between r and r+dr (m^{-2})
r_{max} and r_{min}: maximum and minimum radii of droplet (m)

The total heat flux includes the heat transfer resulting from the phase change and the presence of non-condensable gas. It has been reported that the main resistance from heat transfer comes from the presence of non-condensable gas[19,20,21]. The relationship between total heat flux and condensation rate can be stated in the following way (7):

$$Q = Q_g + Q_c = h_g \times \left(T_b^g - T_i^g\right) + WCR \times H_{fg} \qquad (7)$$

with: Q: Total heat flux (W/m^2)
Q_g: Heat flux through the gas boundary layer (W/m^2)
Q_c: Latent heat flux released by the phase change (W/m^2)
h_g: Heat transfer coefficient in the gas boundary layer ($W/m^2/K$)
$\left(T_b^g - T_i^g\right)$: Temperature difference between the bulk and the vap/liq interface (K)

[1] Institute for Corrosion and Multiphase Technology, Ohio University
[2] TOPCORP

WCR: Water condensation rate (kg/m^2/s)
H_{fg}: Latent heat of evaporation/condensation (J/kg)

The calculations of the heat fluxes are summarized by Zhang[11] and the approach involves the determination of the heat resistances caused by the presence of non condensable gas, the curvature of the droplet, the vapor/liquid interface, the liquid thickness and the promoter surface itself. Assuming that the shape of the drop is hemispherical, a basic representation of the scenario is shown in FIGURE 4.

The corrosion model follows the same approach developed by Nordsveen[15] and Nesic[16,17] but is adapted to a TLC scenario. The representation of the computational domain is shown in FIGURE 5. The expression for transport of species in the presence of chemical reactions, which is valid both for the liquid in the droplet and the porous film, can be described using the species conservation equation. The equation is simplified by assuming no convection (stagnant droplet or droplet sliding in laminar flow) and by considering the effect of migration to be insignificant. The overall species conservation equation in the droplet becomes (8):

$$\frac{\partial \varepsilon C_i}{\partial t} = D_i \frac{\partial^2 (\kappa C_i)}{\partial t^2} + \varepsilon R_i \tag{8}$$

With C_i: concentration of species i,
ε and κ: volumetric porosity and surface permeability of the film respectively (both equal to 1 outside the corrosion product layer),
D_i: Molecular diffusion of species i,
R_i: source or sink of species i,
t: time,
x: special coordinate.

The calculation of the porosity ε and the overall film growth is evaluated through a mass balance conducted on $FeCO_3$ and by using the Van Hunnik[4] equation for the $FeCO_3$ dissolution/precipitation rate (9).

$$\frac{\partial \varepsilon}{\partial t} = -\frac{M_{FeCO_3}}{\rho_{FeCO_3}} R_{FeCO_3} \tag{9}$$

With M_{FeCO3}: Iron carbonate molecular weight (kg/mol)
ρ_{FeCO3}: Iron carbonate density (k/m^3)
R_{FeCO3}: Iron carbonate precipitation rate (mol/m^3/s)

The calculation of the flux of species active in the corrosion reactions are calculated with the following equation (10):

$$N_j = -\frac{i_j}{n_j F} \tag{10}$$

With i_j: current density for species j (A/m^2)
n_j: number of electrons exchanged for species j
F: faraday number (A.s/mol)
N_i: Flux of species j (mol/m^2/s)

Fundamental rate equations of electrochemistry relating the current density "i" to the potential at the metal surface E via an exponential relationship are used for each corrosive species (11):

$$i = \pm i_0 \cdot 10^{\pm \frac{E - E_{rev}}{b}} \quad (11)$$

With i_0: exchange current density,
E_{rev}: reversible potential,
b: tafel slope.

The main equations presented above constitute a set of non-linear coupled differential equations and are solved together using proper numerical methods. A typical simulation result obtained with the version 3 of the selected model is shown in FIGURE 6. Once again, the reader is invited to look at the original publication[11].

Since its first release in 2007, the focus of the software development has been on comparison with field data. The selected model has been consequently updated and the version of the software used in the present study is the version 3.0. The changes involve:

- The implementation of a adapted corrosion model for situations where the droplets of condensed water slide at the top of the line and form a flowing thin film,
- An update in the way the corrosion product film porosity is calculated at a low condensation rate,
- The implementation of additional resistance to heat transfer on the outside of the pipe depending on the type of environment (sea, river, air).

The selected model also has known limitations, some of them being the subject of on-going research activities. These limitations are listed below:

- No condensate chemistry calculation is included in the model. It is assumed that only the water vapor condenses.
- The influence of hydrogen sulfide on the TLC rate is incorporated in the model but not validated.
- The model assumes that the flow lines are horizontal and that the flow regime is stratified.
- The potential for corrosion inhibition provided by pigging implementation is considered nil and the droplet transport is assumed non-existent.

Scope of the present work

Although a lot of progress has been achieved over the past 10 years on the understanding of the sweet TLC mechanism and its prediction, almost all the work published is based on experimental work performed in laboratory. The selected model was based on data obtained in large (4"ID) scale flow loop tests with an exposure time of 3 weeks[22] It is expected that the TLC rates observed in the field over periods of years can be rather different from experimental data obtained over shorter time periods. In addition, field conditions are notoriously uncertain and the accuracy of the inspection tools can be reduced significantly by the pipeline conditions (scale formation, efficiency of the cleaning method …). Also for the pipelines subject to TLC the accuracy of some inspection tools is quite low[23].

PIPELINE DATA AND OPERATING CONDITIONS

The field consists of eleven different flow lines (Line A to line K) operating at various operational conditions. Typical operating conditions in Bongkot sealines are given in Table 1. TABLE

2 presents a set of three conditions representing the operational life of each line. These three conditions are labelled high, medium and low and stand for a set of field parameters (total pressure, CO_2 gas content, temperature, flow rate) at their highest, most average and lowest values. It should be stressed only the medium condition is representative of a state of the production at one point in time (average production). The other two conditions, low or high, describe the lowest or highest values obtained for each parameter during the entire life of the pipeline but theses conditions were not encountered in the pipeline at the same time. For example, the highest gas temperature was probably measured together with the highest flow rate but not with the highest pressure (typically, high flow rates are encountered at lower pressure). Therefore, the TLC simulations presented in the next chapter exclusively focus of a set of medium level conditions for each line.

The lines are 14" (0.356 m), 15" (0.381 m) or 16" (0.406 m) pipe diameter with a wall thickness of 15.9mm or 20.6mm including about 10 mm of corrosion allowance. All the lines are coated with three layers polypropylene coating but only four of them (lines F, H J and K) have additional concrete coating (25.4 mm thick). At field joints, there is no polyurethane foam infill. A description of the line characteristics is displayed in TABLE 3.

Finally, the results form the MFL inspections are shown in TABLE .

SIMULATION RESULTS AND INTERPRETATION

FIGURE 7 presents the conditions used in the simulations. The simulations were run until a steady state corrosion rate was achieved (no significant change of corrosion rate over time).

Simulation Results

The results obtained with the selected model are shown in FIGURE 8 which shows the predicted condensation and TLC rates. Since the selected model is a mechanistic model, the differences in the predicted corrosion rates between each flow line can be directly related to the difference in the value of most influencing field parameters. First, all the lines have similar pipe diameters, pipe wall thicknesses and insulation characteristics. The outside environment is the sea water at 25°C and none of the lines are buried. Therefore the severity of top of the line corrosion depends only on the following parameters: gas temperature, gas velocity and partial pressure of CO_2. Furthermore, FIGURE 8 and FIGURE 7 should be used together so that the reader can easily correlate the change in corrosion rate with an actual change in the field conditions (temperature, gas velocity etc …).

As a general comment, the flow line average conditions are very aggressive. The inlet gas temperature is usually between 70 and 95°C, the gas velocity can reach 8 m/s and the CO_2 content is between 3.5 and 11 bars. Since the flow lines sit on the sea bed and do not have any special heat insulation, the predicted water condensation rate is always quite high (around 1.5 ml/m^2/s). In these conditions, TLC is expected to be quite severe. The following shows a more detailed line by line analysis of the predictions.

Line A shows a relatively low TLC rate mainly because the difference between the fluid temperature and the outside environment is small and because the gas velocity is moderate (3.2 m/s) leading a low condensation rate (0.25 ml/m^2/s). Low condensation rates are usually associated with the formation of more protective corrosion product scales (made of $FeCO_3$) and lower TLC rates. However, the partial pressure of CO_2 is quite high (9.5 bars) making the environment still quite corrosive.

In comparison, line B presents a higher gas velocity and gas temperature leading to a much higher rate of heat transfer with the outside environment and a very high condensation rate (3.4 ml/m^2/s).

The CO_2 content being similar, the TLC rate for line B is predicted at 5 mm/year and is logically higher than line A.

Following the same method, line C and D which show moderate gas temperature but lower gas velocity heading to significantly lower condensation rates (0.5 to 1 ml/m^2/s) than line B. The CO_2 content being much smaller, the conditions should lead to lower TLC rates (1.8 mm/year for line C and 1.2 mm/year for line D).

Line E shows a set of quite aggressive conditions with high gas temperature (90°C), gas velocity (8 m/s and CO_2 content (8 bars). Higher gas velocity not only enhances the heat transfer and consequently the condensation rate but also changes the condensation pattern from stagnant to sliding droplets. Actually, the droplets of condensed water are predicted to be sliding at the top of the pipe in all the conditions of the Bongkot field. The speed of these droplets depends on the friction with the gas phase and therefore with the gas velocity (the higher the gas velocity, the faster the droplet will slide). The corrosion reactions would be enhanced by higher sliding velocity since the resistance to mass transfer can be considerably decreased.

Line F shows similar conditions to line E except for the CO_2 content which is a little bit smaller. However, line F is equipped with concrete coating and consequently shows consequently a lower condensation rate (1.5 ml/m^2/s for line F and 2.8 ml/m^2/s for line E). The TLC rate is logically predicted at a lower value (2 mm/year for line F and 3 mm/year for line E). At field joints, the corrosion rates can be higher than at concrete coated sections as there is no polyurethane foam infill at field joints. A further analysis is needed considering the field joints area as cold spots.

Line G is very comparable to line E and shows a similar water condensation rate and TLC rates.

Line H is a little bit peculiar. The presence of concrete coating on this line leads to a lower condensation rate (1.8 ml/m^2/s) when compared with lines E or G. However, this value is still significant. Coupled with a higher gas velocity, the TLC rates are predicted at a value of 4.2 mm/year. Here the effect of the gas velocity seems to be predominant. The corrosion rates would be more severe at field joints.

Line I shows a lower gas velocity (and consequently a lower condensation rate) but a much higher CO_2 content. These two parameters seem to balance each other and lead to a predicted TLC rate comparable to line E or G.

Finally, lines J and K are both equipped with concrete coating and show lower condensation rates especially for line K which has in addition a moderate gas temperature (65°C). Line J and F are somehow comparable both in terms of conditions and TLC rates. In the same way, Lines K and C are also quite similar.

In addition, the same results are presented in a different way in FIGURE 9 to FIGURE 12. The analysis of these graphs is not straight forward and requires clarification. The objective is to extract some indications of the influence of each of the main parameters (gas velocity, partial pressure of CO_2, gas temperature and condensation rate) on the predicted TLC rate. Each graph plots the TLC rates predicted for each of the eleven flow lines at low, medium and high conditions (these three data pints forming the plotted lines). The TLC rate obtained for low conditions is lower than the one obtained for medium conditions which are also always lower than the one calculated for high conditions; it is therefore quite easy to identify which TLC rate corresponds to which condition for a specific flow line The data point on the left, middle and right of each plotted line corresponds to low, medium and high conditions respectively. Once again, the low and high conditions do not correspond to an actual combination of field conditions as it is explained earlier. In addition, although these kind of figures provide interesting information, they can be very misleading: it could be understood that the changes in corrosion rates are only due to only the one specific parameter presented in the

graph (condensation rate or pCO_2 or gas temperature or gas velocity) which is not correct. In addition, an oversimplified interpretation of the effect of these field parameters could be easily drawn from the figures. This is why the values of the predicted TLC rates or of the selected parameters are not shown, the objectives being to extract trends and not artificial threshold values.

Below are a few comments that can be extracted from the graphs:

- The influence of the gas temperature is quite clear (FIGURE 9). In the case of the Bongkot field, heat insulation is not very effective and high fluid temperature leads to usually high water condensation rates. The predicted TLC rates are consequently quite high if the gas temperature is above 50°C. However, high gas temperature associated to effective heat insulation might not lead to TLC issues if the condensation is kept low.
- The gas velocity does greatly affect the TLC rate (FIGURE 10). The condensed water tends to form droplets which slide on the pipe wall at relatively high velocity. This leads to much higher corrosion rates when compared with stagnant droplets or slow moving droplets scenarios (the mass transfer of corrosive species being enhanced). On the right hand side of the graph (where the gas velocities are the highest) the flow regime can be closed to non-stratified flow (annular flow) which is expected to create severe corrosion problems if bottom of the line inhibition is not applied.
- The partial pressure of CO_2 seems to have a somehow linear relationship with the predicted corrosion rate (FIGURE 11). The higher pCO_2, the higher the TLC rate. However, the corrosive effect of high partial pressure of CO_2 can be attenuated by low condensation rate and low gas velocity.
- Finally, the influence of the water condensation rate is shown in FIGURE 12. The TLC rate does not seem to be exactly proportional the value of water condensation rate. According to the software predictions, moderate or high condensation rates lead to equally high TLC rates. Only very low values of condensation rate associated to low pCO_2 and low gas velocity provide manageable TLC rates.

Comparison With MFL Measurements

The MFL results from TABLE are converted to mm/y and shown in FIGURE 13 together with the predicted TLC rates obtained for medium conditions (which are the conditions most representative of the operational life of the flow lines) with the selected model. It is understood that MFL results are highly inaccurate. Stabilized corrosion rates, which are based on to consecutive MFL runs, makes the analysis more difficult. Finally actual MFL readings are used for the present analysis.

Corrosion rate predictions obtained with the selected model are within 50% of the MFL data (first inspection) in 9 out of 11 flow lines. In the remaining two flow lines (line B and C), the corrosion rates can be over predicted by a factor of 5. Overall, the selected model prediction trend follows the MFL results trend which is quite encouraging. However, the TLC rates are in general still too conservative.

In the case of line B, the operational conditions are the most aggressive of the entire Bongkot field and high TLC rates are expected. However, the selected model predicts a TLC rate of 5 mm/year while MFL results are between 1.23 and 1.8 mm/year. The reason behind the discrepancy is not clear.

In the case of line C which shows lower CO_2 content, lower velocity and lower temperature than line B, the MFL inspection gave TLC rates between 2.2 and 3.8 mm/year compared to a selected model prediction of 0.7 mm/year. Once again, this discrepancy is not expected.

For comparison purposes, the TLC rates predicted by DeWaard's[2] correlation are shown in FIGURE 14 together with selected model predictions and MFL data. To DeWaard's credit, the correlation

developed in 1991 does follow for the most part the same trend as the selected model. It also overestimates the MFL data but by a bigger extent compared to selected model (Line B and C are still not predicted correctly). It is actually not surprising that DeWaard's correlation seems to catch more or less accurately the corrosion behaviour in the specific conditions of the Bongkot field. As it is presented earlier in this paper, the correlation depends exclusively on the partial pressure of CO_2 and the gas temperature. DeWaard's correlation predictions are the closest to MFL data when the influence of these two parameters is dominant. The Bongkot field conditions are very aggressive and in many cases the water condensation rate is so high that he does not influence any more the extent of the corrosion attack. However, when the gas velocity or the condensation play a bigger role (Line F, I, J), the correlation predictions deviate from MFL data to a larger extent. DeWaard's correlation is consequently not expected to predict well TLC rates in well insulated lines where the water condensation rate is a primary parameter.

Comments About Predicted and Measured Values

Possible origins of the discrepancies

Some discrepancies exist between predicted and measured corrosion rates. However, the fact that a prediction model does not accurately predict the field results does not mean the prediction is not correct[24, 25]. In fact the production parameters change during field life and also the corrosion rate is not linear in time. When corrosion rates are calculated using MFL results, it is assumed that the corrosion rate is the same at the beginning of production and when the pipe is inspected. The field experience from Bongkot showed that this is not true (Table 4). For example, clustering of small pits creating large corroding surfaces (and reducing the corrosion rates) is observed in several pipelines. Some companies providing intelligent pigging service now take into account the stabilization mechanism and recent intelligent pigging results by MFL are much more accurate than a few years ago. Another problem is that metallurgical aspects are ignored in the prediction models (for example carbon steels of similar grades produced from different suppliers are subject to different corrosion rates).

There are also some mechanisms, affecting the corrosion processes in the pipelines, which have not yet been taken in into account in prediction models.

1. Regarding the flow velocity effect on the behavior of water film/ droplets, some field observations have shown that if the gas velocity is too low, water droplets may remain at the 12 o'clock position causing some sort of "water line corrosion" leading to line leaks.
2. Concrete coated pipes of Bongkot have no polyurethane infill at field joints areas. At field joints high water condensations and corrosion rates are expected as these locations work like cold spots. This aspect was not taken into account in above analysis.

Main purpose of corrosivity prediction

Accurate corrosivity prediction does not mean necessarily prediction of accurate corrosion rates. What is expected from testing of a model (in the present case testing of the selected model in Bongkot field case) is the confirmation that the model could successfully predict an experienced problem and its importance (in the present case high and low thickness losses due to TLC). If this is confirmed, then the model can be used for the prediction of specific problems and for corrosion studies (for example in case of TLC, prediction of cold spot corrosion[1], determining priorities for inspection and evaluation of TLC risk for new field development projects).

Future Development

In sweet conditions, Top of the Line Corrosion is encountered where the heat exchange with the surrounding environment is the highest. This is why TLC is often the worse at the beginning of a line

and tends to decrease in intensity as the fluid cools down further down the pipe. So far, the present study focuses on a "medium case" situation for which the conditions are not encountered at the same location and the same time. This situation brings consequently added uncertainties. It would be in fact very valuable to be able to link ILI data for a specific location in the pipe with a set of field conditions (temperature, pressure, gas velocity). Profiles and temperature and pressure along the line could be used to generate TLC predictions which could then be compared more directly with MFL results on actual features. Variations of these profiles with time should be incorporated in the study as production rates often vary quite a lot.

CONCLUSIONS

- Information available from the Bongkot field is sufficient to successfully conduct an analysis for TLC evaluation.
- When comparing field data and predicted corrosion rates it is important to keep in mind the relatively low accuracy of the measurement method and decrease of corrosion rates during the field life.
- Since the selected model is a mechanistic model, the differences in the predicted corrosion rates between each flow line can be directly related to the difference in the value of field parameters such as condensation rate, pCO_2, gas temperature, and gas velocity.
- Selected model predictions of the eleven flow lines of the Bongkot field data are quite encouraging (the risk of TLC and its relative importance in the Bongkot sealines is predicted quite well) but still too conservative.
- Selected model can be still improved but the prediction of actual corrosion rates in the pipelines can not be a short term objective.
- In the case of Bongkot field, more analysis is needed at field joints for concrete coated pipes.

ACKNOWLEDGEMENTS

Authors would like to thank the PTTEP management for their permission to publish this paper.

REFERENCES

1. Gunaltun Y. Punpruk S., Thammachart M., Tanaprasertsong P., "Worst case TLC: cold spot corrosion", Corrosion /10 Paper # 14337
2. DeWaard C., Lotz U., Milliams D.E., "Predictive model for CO2 corrosion engineering in wet natural wet gas pipelines", Corrosion, 47(12), p 976-985, 1991.
3. Pots B.F.M., Hendriksen E.L.J.A., "CO_2 corrosion under scaling conditions – The special case of top-of-the-line corrosion in wet gas pipelines", Corrosion/00, paper# 31.
4. Van Hunnik E.W.J., Pots B.F.M., Hendriksen E.L.J.A., "The formation of protective $FeCO_3$ corrosion product layers in CO_2 corrosion", Corrosion/96, paper# 6.
5. Vitse F., Gunaltun Y., Larrey de Torreben D., Duchet-Suchaux P., "Mechanistic model for the prediction of top-of-the-line corrosion risk", Corrosion/03, paper# 3633.
6. Vitse F., Khairul A., Gunaltun Y., Larrey de Torreben D., Duchet-Suchaux P., "Semi-empirical model for prediction of the top-of-the-line corrosion risk", Corrosion/02, paper# 2245.
7. Vitse F., "Experimental and theoretical study of the phenomena of corrosion by carbon dioxide under dewing conditions at the top of a horizontal pipeline in presence of a non-condensable gas", Ohio University, PhD Dissertation, 2002.
8. Gunaltun Y., Larrey D., "Correlation of cases of top of the line corrosion with calculated water condensation rates", Corrosion/00, paper# 71.
9. Nesic S., Postlethwaite J., Olsen S., "An Electrochemical Model for Prediction of Corrosion of Mild Steel in Aqueous Carbon Dioxide Solutions", Corrosion, 52(4), p 281-294, 1991.

10. Nyborg R., Dugstad A., “Top of the line corrosion and water condensation rates in wet gas pipelines”, Corrosion/07, paper# 7555.
11. Zhang Z., Hinkson D., Singer M., Wang H., Nesic S., “A mechanistic model for Top of the line corrosion”, Corrosion, 63(11), 1051-1062, 2007.
12. Remita E., Tribollet B., Sutter B.,Ropital F., Longaygue X., Kittel J., Taravel-Condat C., Desamaise N.,“A kinetic model for CO2 corrosion in confined aqueous environments”, Journal of the Electrochemical Society, 155(1), C41-C45, 2008.
13. Amri J.,, Gulbrandsen E., Nogueira R.P., “The effect of acetic acid on the pit propagation in CO2 corrosion of carbon steel”, Electrochemistry Communications, 10, 200–203, 2008.
14. Hinkson D., Singer M., Zhang Z., Nesic S., “A study of the chemical composition and corrosivity of the condensate in top of the line corrosion”, Corrosion/08, paper# 8466.
15. Nordsveen N., Nesic S., Nyborg R., Stangeland A.,“A Mechanistic Model for Carbon Dioxide Corrosion of Mild Steel in the Presence of Protective Iron Carbonate Films - Part 1: Theory and verification”, Corrosion, 59(05), 443-456, 2003.
16. Nesic S., Nordsveen N., Nyborg R., Stangeland A.,“A Mechanistic Model for Carbon Dioxide Corrosion of Mild Steel in the Presence of Protective Iron Carbonate Films - Part 2: A numerical experiment”, Corrosion, 59(06), 489-497, 2003.
17. Nesic S., Nordsveen N., Nyborg R., Stangeland A.,“A Mechanistic Model for Carbon Dioxide Corrosion of Mild Steel in the Presence of Protective Iron Carbonate Films - Part 3: Film growth model”, Corrosion, 59(07), 616-628, 2003.
18. Rose J.W., “Dropwise condensation theory and experiment: a review”, Proceedings Institute of Mechanical Engineers, vol.216, Part A: Journal of Power and Energy, 2002, 115-128.
19. Tanner D.W., Potter C.J., Pope D., West D., “Heat transfer in dropwise condensation – Part1 & 2”, International Journal of Heat and Mass Transfer, Vol.8, 419-426 & 426-436, 1965.
20. Wang C.Y., Tu C.J., “Effect of non-condensable gas on laminar film condensation in a vertical tube”, International Journal of Heat and Mass Transfer”, Vol.31, #11, 2339-2345, 1988.
21. Wang S., Utaka Y., “Effect of non-condensable gas mass fraction on condensation heat transfer for water-ethanol vapor mixture”, JSME International Journal, Series B, Vol.47, #2, 2004.
22. Singer M., Nesic S., Hinkson D., Zhang Z., Wang H., “CO_2 top of the line corrosion in presence of acetic acid - A parametric study”, Corrosion/09, paper# 9292.
23. Gunaltun Y. Piccardino R, Vinazza D. “Interpretation of MFL and UT inspection results in case of top of line corrosion”, Corrosion /06 Paper # 06170.
24. Gunaltun Y., Han de Reus J.M., Nyborg R.,”The reliability of laboratory and field parameters used in the prediction models”, Corrosion/03, Paper # 03622.
25. Gunaltun Y., Kopliku A.,” Collection of reliable field data for validation of prediction models”, Corrosion/06, Paper # 06117.

TABLES

TABLE 1: TYPICAL OPERATING CONDITIONS

CO_2	20 to 33 %
H_2S	< 20 ppm
Pipeline inlet temperatures	80 – 105 ^oC
Pipeline inlet pressures	35- 40 bars
Gas production rate	28 to 80 MMscf/d (0.793 to 2.27 MMcm/d)
Condensate production rate	200 to 900 bbls/d (31.75 to 142.86 m3/d)
Water production rate	1400 to 1800 bbls/d (222.22 to 285.71 m3/d)

TABLE 2: BONGKOT FIELD CONDITIONS

Line	Condition	Temperature (c)	P total (bar)	pCO_2 (bar)
A	High	85	39	17.78
	Medium	50	32	9.63
	Low	30	11	0.59
B	High	101	33	14.72
	Medium	90	28	9.74
	Low	59	24	4.15
C	High	86	36	7.92
	Medium	66	28	3.79
	Low	35	24	0.45
D	High	92	33	12.87
	Medium	76	29	6.17
	Low	39	22	3.11
E	High	94	35	12.18
	Medium	88	30	7.65
	Low	76	23	3.29
F	High	93	42	19.55
	Medium	88	31	5.31
	Low	78	25	2.51
G	High	94	41	17.63
	Medium	88	30	8.13
	Low	75	23	2.94
H	High	105	49	12.57
	Medium	94	37	6.79
	Low	51	17	1.71
I	High	107	53	17.16
	Medium	91	42	11.22
	Low	46	18	3.17
J	High	105	40	9.39
	Medium	95	32	6.16
	Low	67	3	0.40
K	High	91	39	7.18
	Medium	68	29	2.74
	Low	N/A	N/A	N/A

TABLE 3: SEALINES CHARACTERISTICS

	Internal diameter (inch)	Steel conductivity (W/m/K)	Steel thickness (mm)	Coating conductivity (W/m/K)	Coating thickness (mm)	Concrete conductivity (W/m/K)	Concrete thickness (mm)
A	13.4	60.13	15.9	0.22	2	-	-
B	13.4	60.13	15.9	0.22	2	-	-
C	17.2	60.13	20.6	0.22	2	-	-
D	17.2	60.13	20.6	0.22	2	-	-
E	17.2	60.13	20.6	0.22	2	-	-
F	15.4	60.13	15.9	0.22	2	1.5	25.4
G	13.4	60.13	15.9	0.22	2	-	-
H	15.4	60.13	15.9	0.22	2	1.5	25.4
I	13.4	60.13	15.9	0.22	2	-	-
J	15.4	60.13	15.9	0.22	2	1.5	25.4
K	15.4	60.13	15.9	0.22	2	1.5	25.4

TABLE 4: MFL RESULTS OBTAINED FOR ELEVEN BONGKOT SEALINES

	Production start up	Pipe thickness (mm)	Inspections Thickness loss (%)	Average C.R. (mm/y)	Stabilised C.R. (mm/y)
Line A	1993	15.9	47 (MFL in 1998)	1.5	1.5
			33 (MFL in 2000)	0.8	< 0.5
Line B	1993	15.9	59 (MFL in 1998)	1.87	1.87
			58 (MFL in 2000)	1.32	< 0.5
Line C	1995	20.6	76 (MFL in 1999)	3.9	3.9
			65 (MFL in 2001)	2.23	<0.5
Line D	1996	20.6	45 (MFL in 2001)	1.85	1.85
Line E	1996	20.6	38 (MFL in 1999)	2.6	2.6
			29 (MFL in 2002)	1	< 0.5
Line F	1997	15.9	33 (MFL in 2001)	1.3	1.3
			59 (MFL in 2004)	1.3	1.3
Line G	1997	15.9	47 (MFL in 2000)	2.5	2.5
			73 (MFL in 2005)	1.45	1.45
Line H	1998	15.9	55 (MFL in 2001)	2.9	2.9
			72 (MFL in 2004)	1.9	1.9
Line I	1998	15.9	43 (MFL in 2002)	1.7	
Line J	2001	15.9	22 (MFL in 2004)	1.16	
Line K	2001	15.9	25 (MFL in 2004)	1.33	

FIGURES

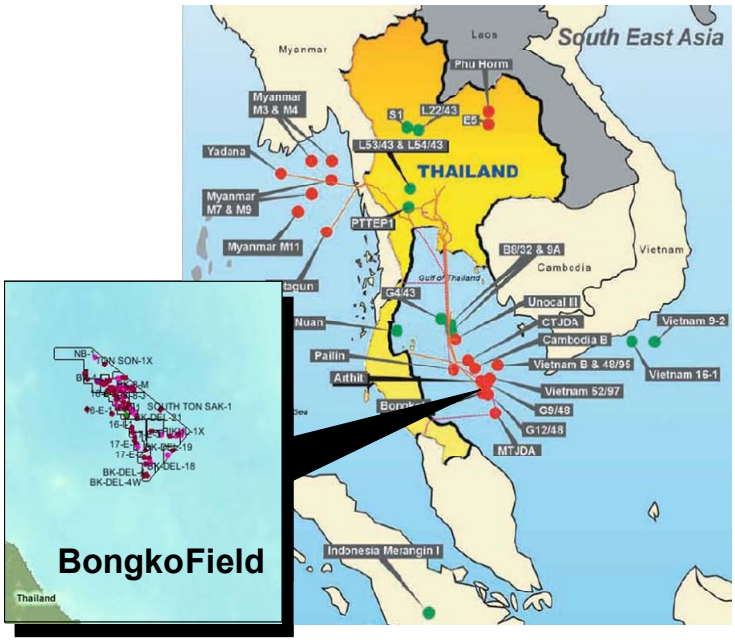

FIGURE 1: Location of the Bongkot field

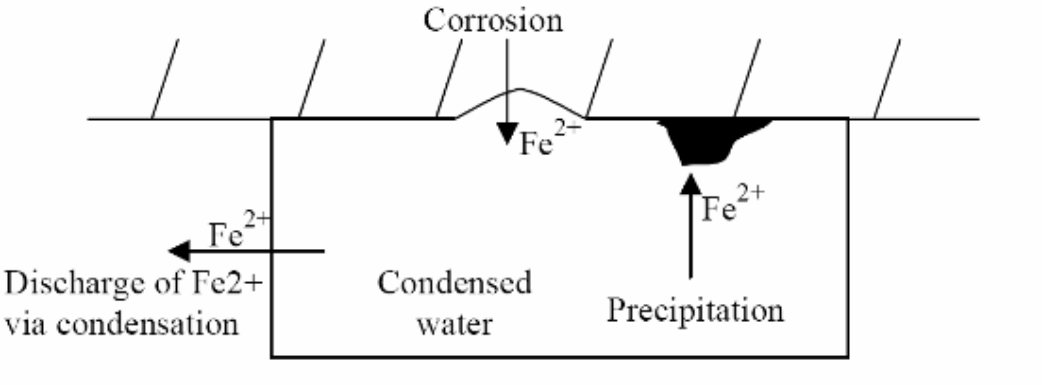

FIGURE 2: Transport, source and sink of Fe^{2+} during TLC[5]

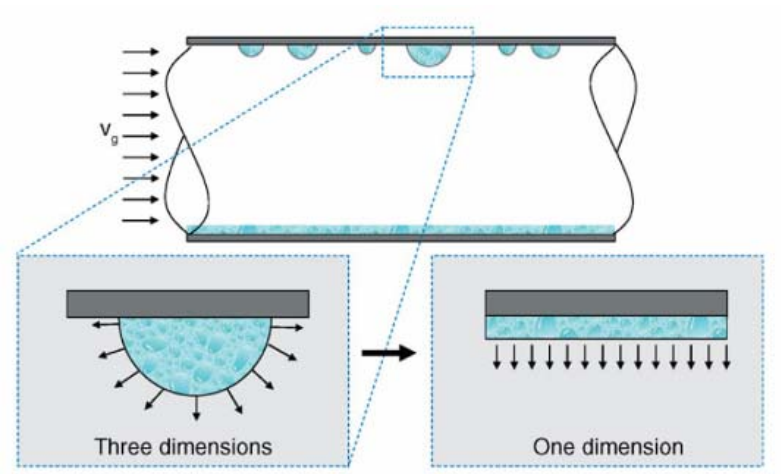

FIGURE 3: The simplification from a 3D (droplet) to 1D (liquid film) approach Error! Reference source not found.

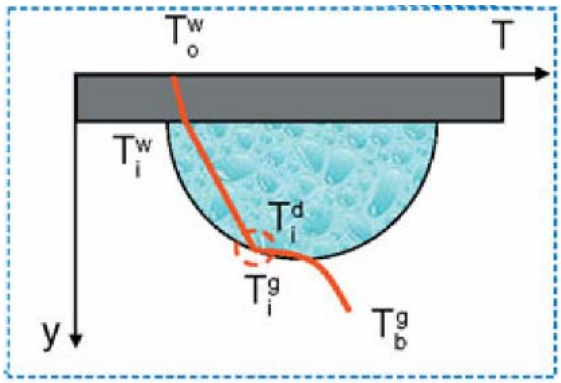

FIGURE 4: Temperature gradient for a single droplet Error! Reference source not found.

(T_o^w: outer promoter temperature; T_i^w: inner promoter temperature; T_i^d: interfacial temperature in the liquid side; T_i^g: interfacial temperature in the gas side; T_b^g: bulk gas temperature)

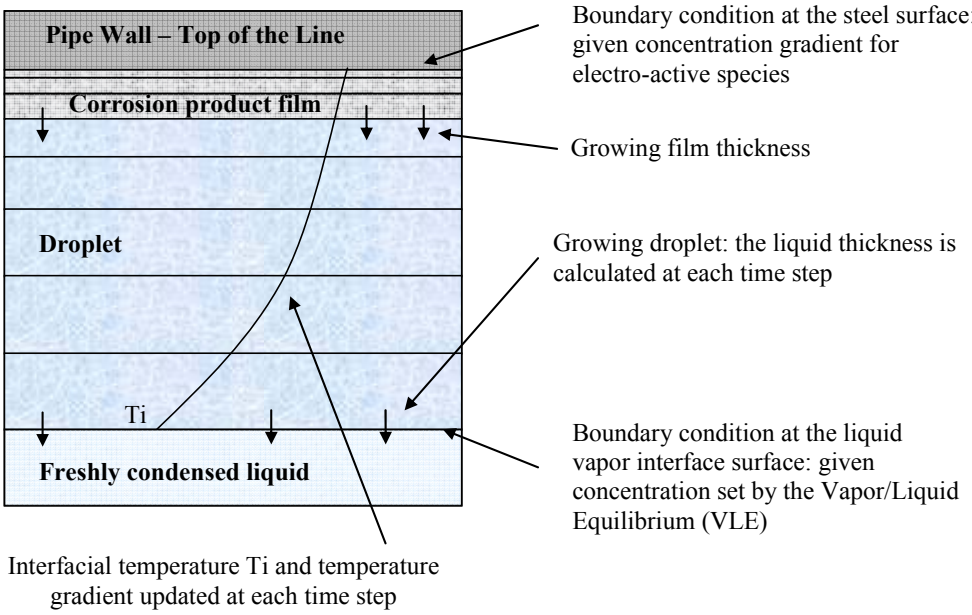

FIGURE 5: Schematic of the corrosion calculations in a growing droplet

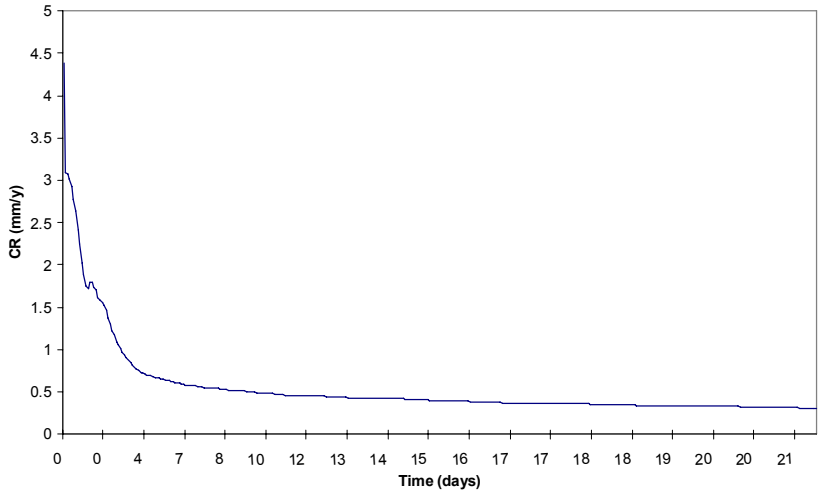

FIGURE 6: Typical TLC rate profile prediction

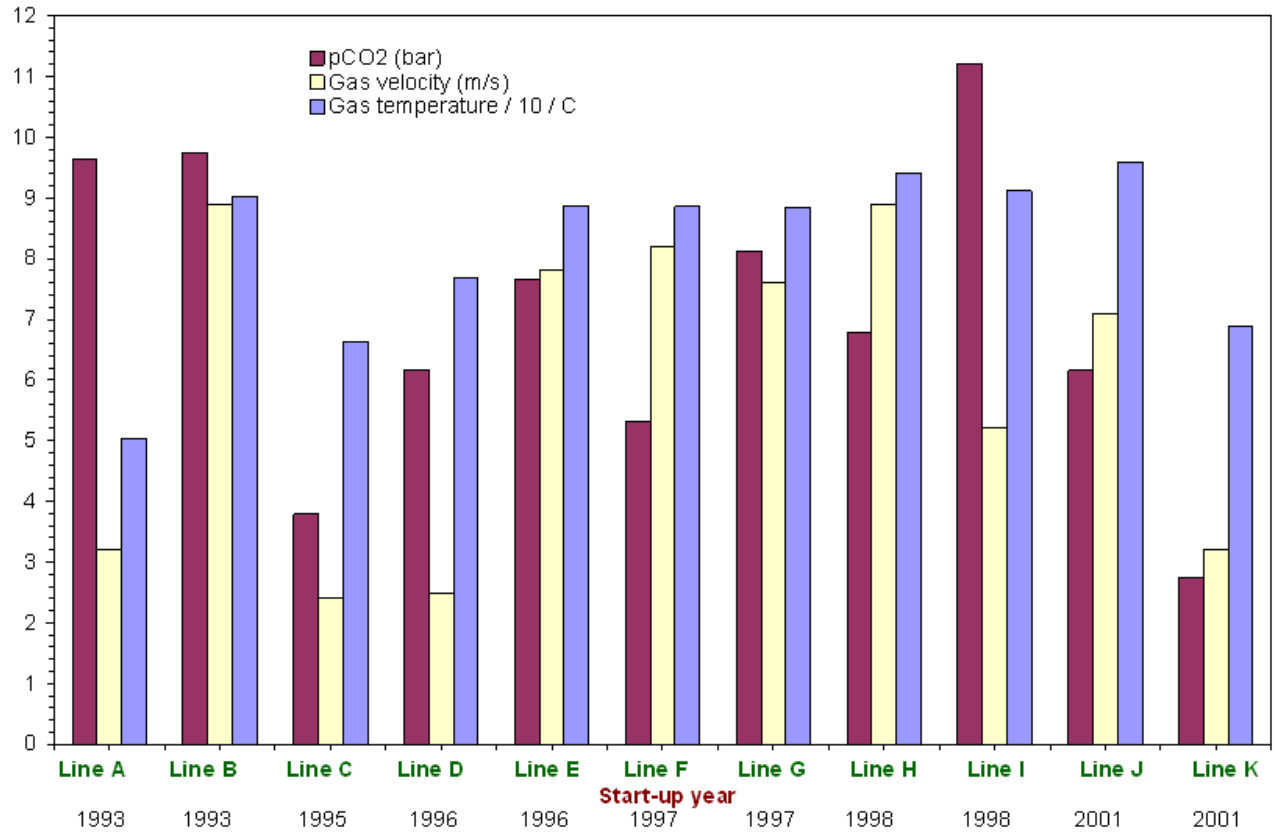

FIGURE 7: Flow line main conditions

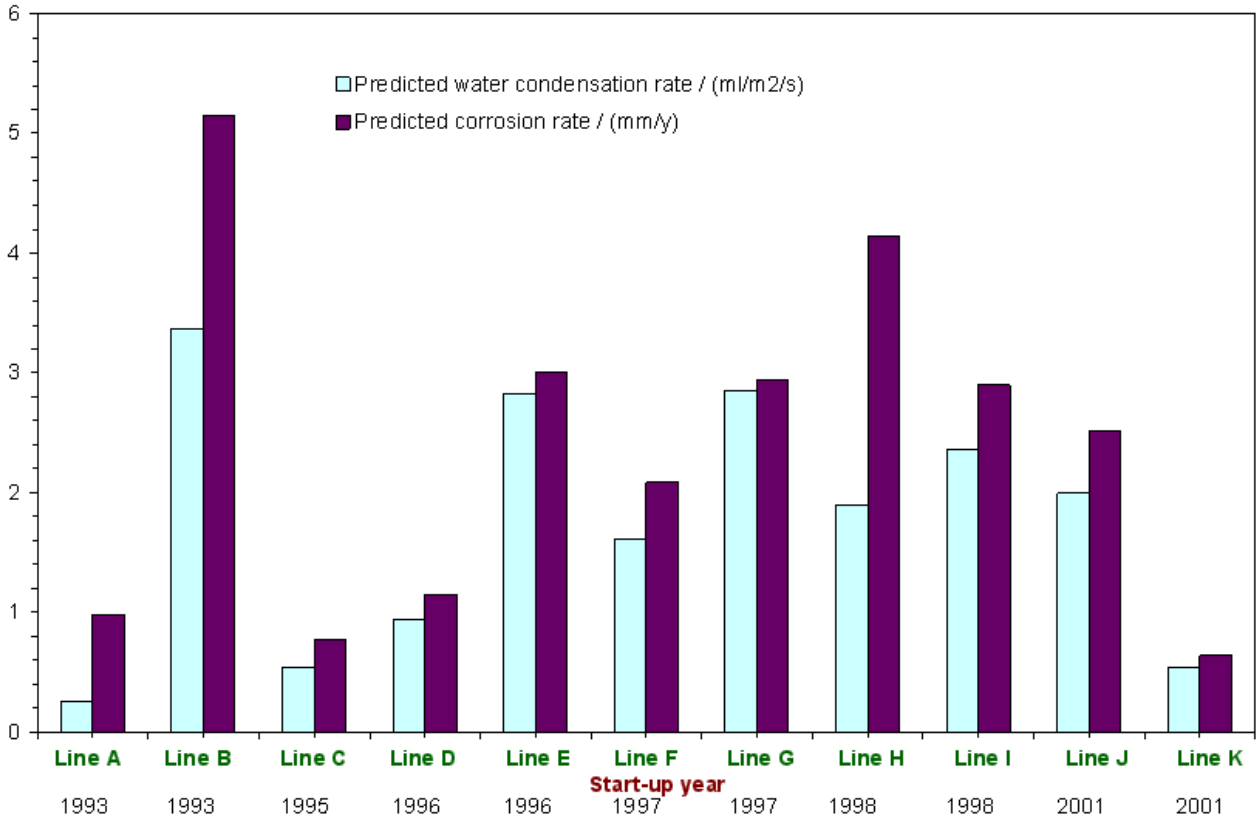

FIGURE 8: Selected model predictions for the water condensation rate and the top of the line corrosion rate

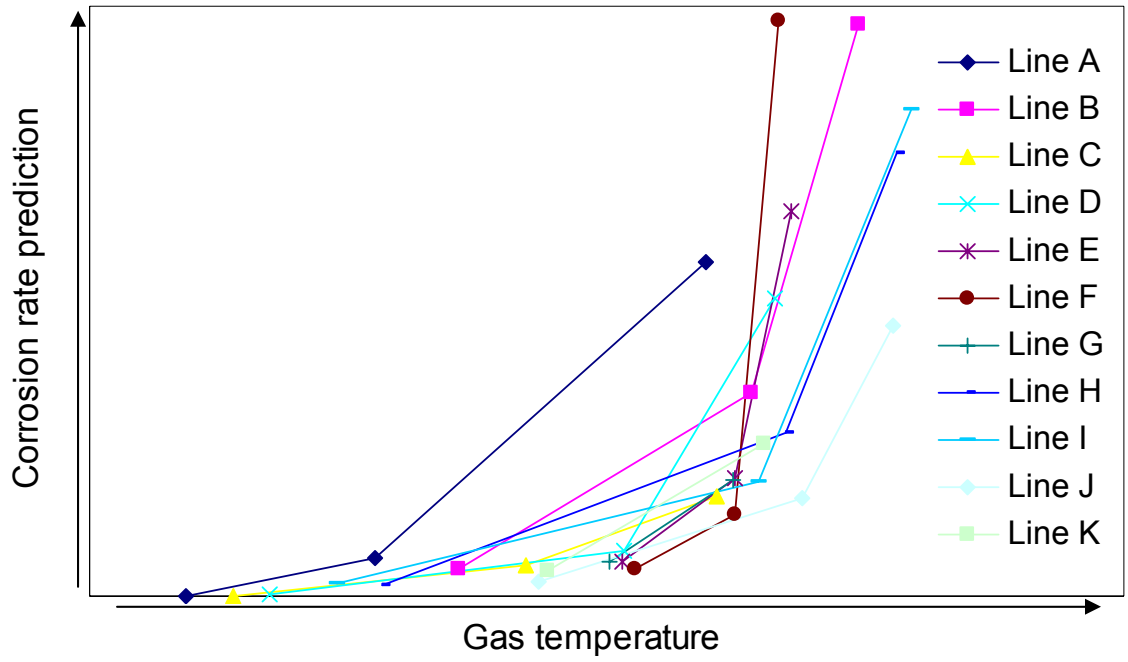

FIGURE 9: Overall influence of the gas temperature on the top of the line corrosion rate

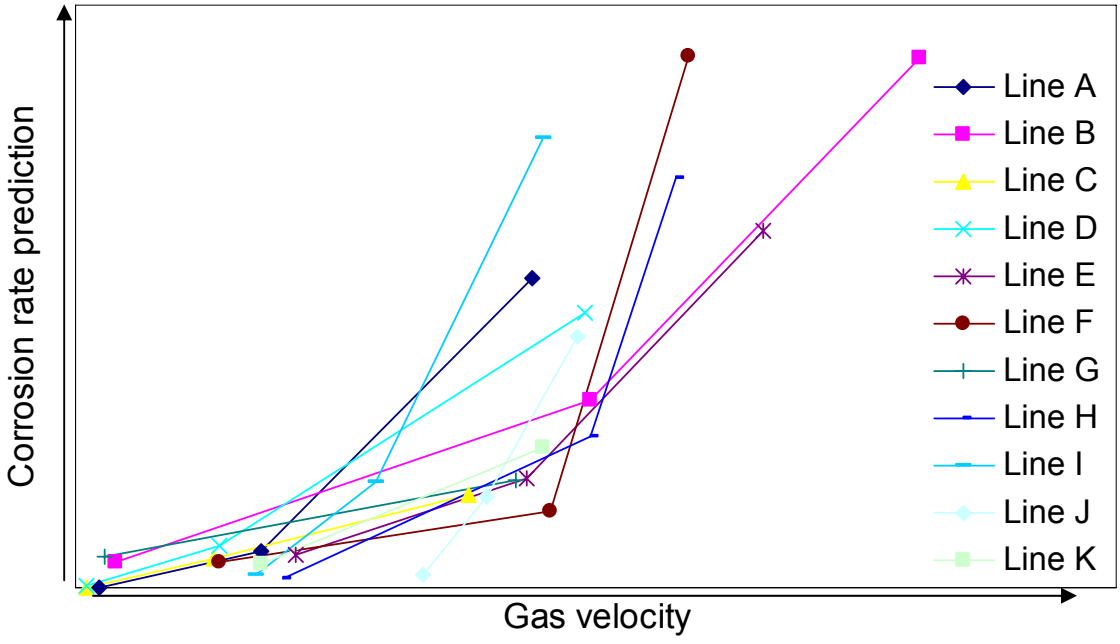

FIGURE 10: Overall influence of the gas velocity on the top of the line corrosion rate

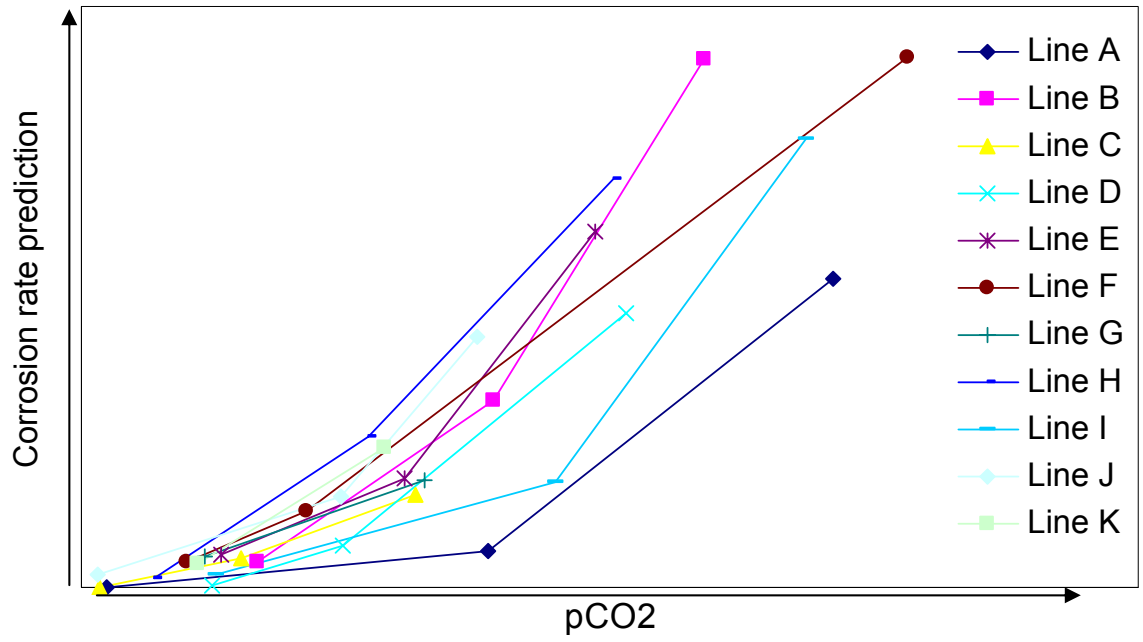

FIGURE 11: Overall influence of the partial pressure of CO_2 on the top of the line corrosion rate

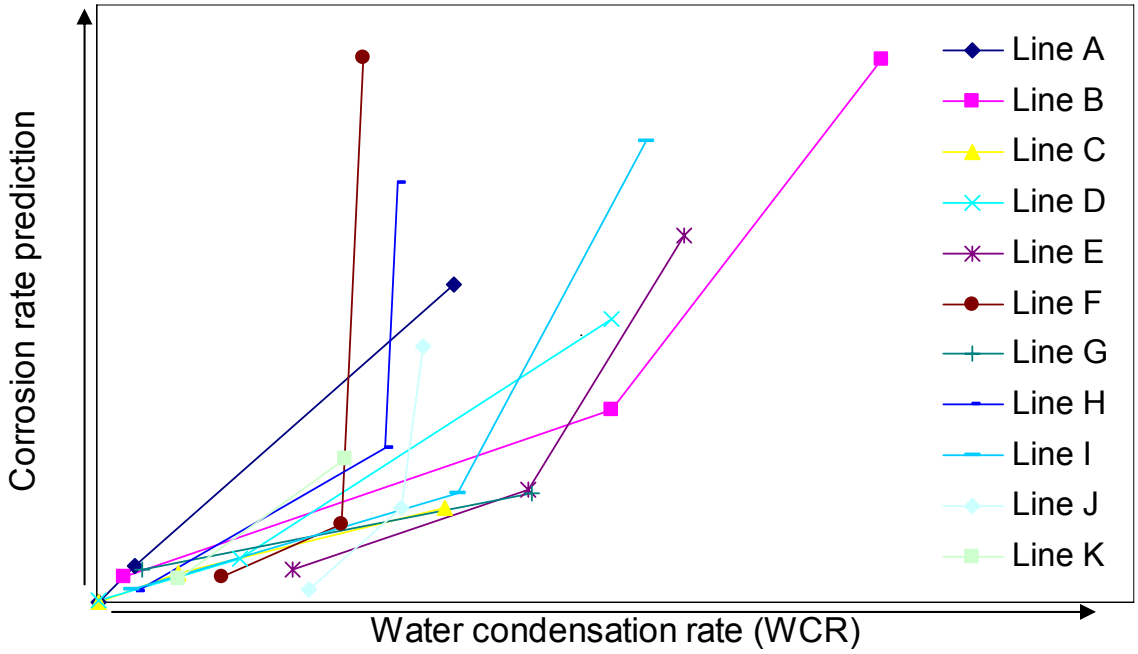

FIGURE 12: Overall influence of the water condensation rate on the top of the line corrosion rate

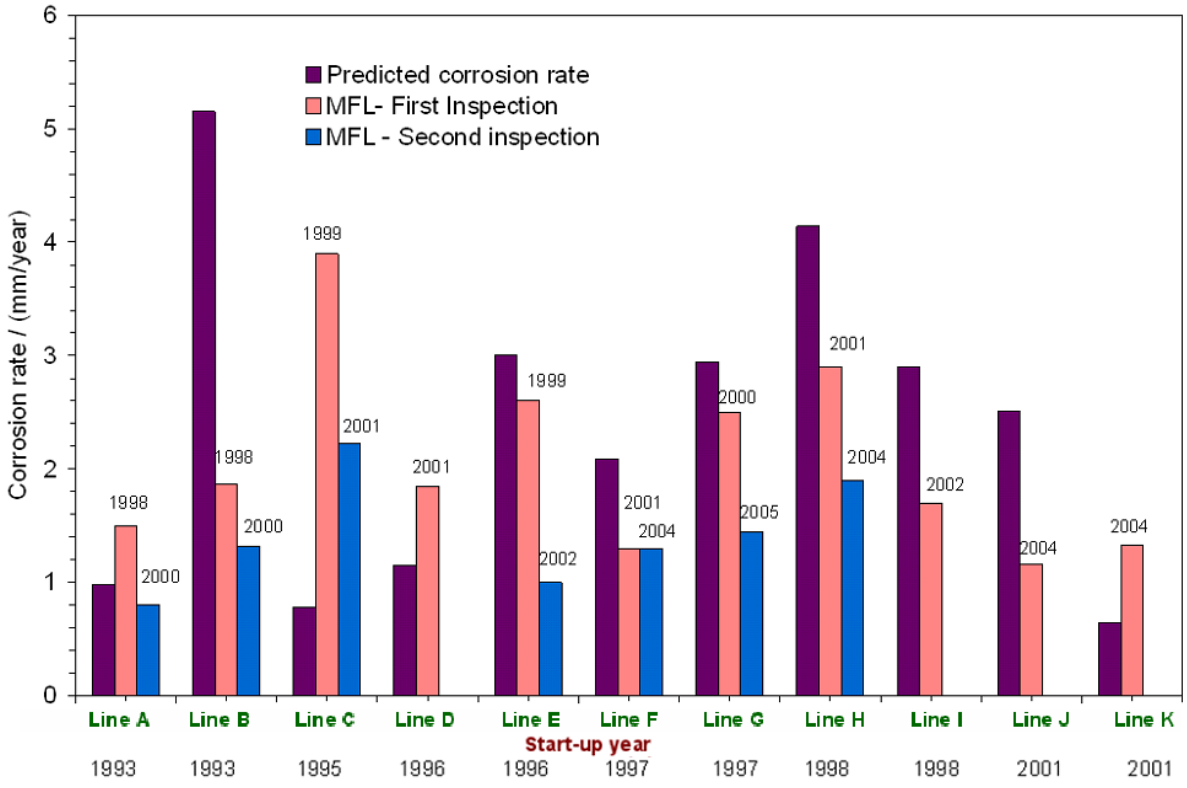

FIGURE 13: Comparison between selected model predictions and MFL data

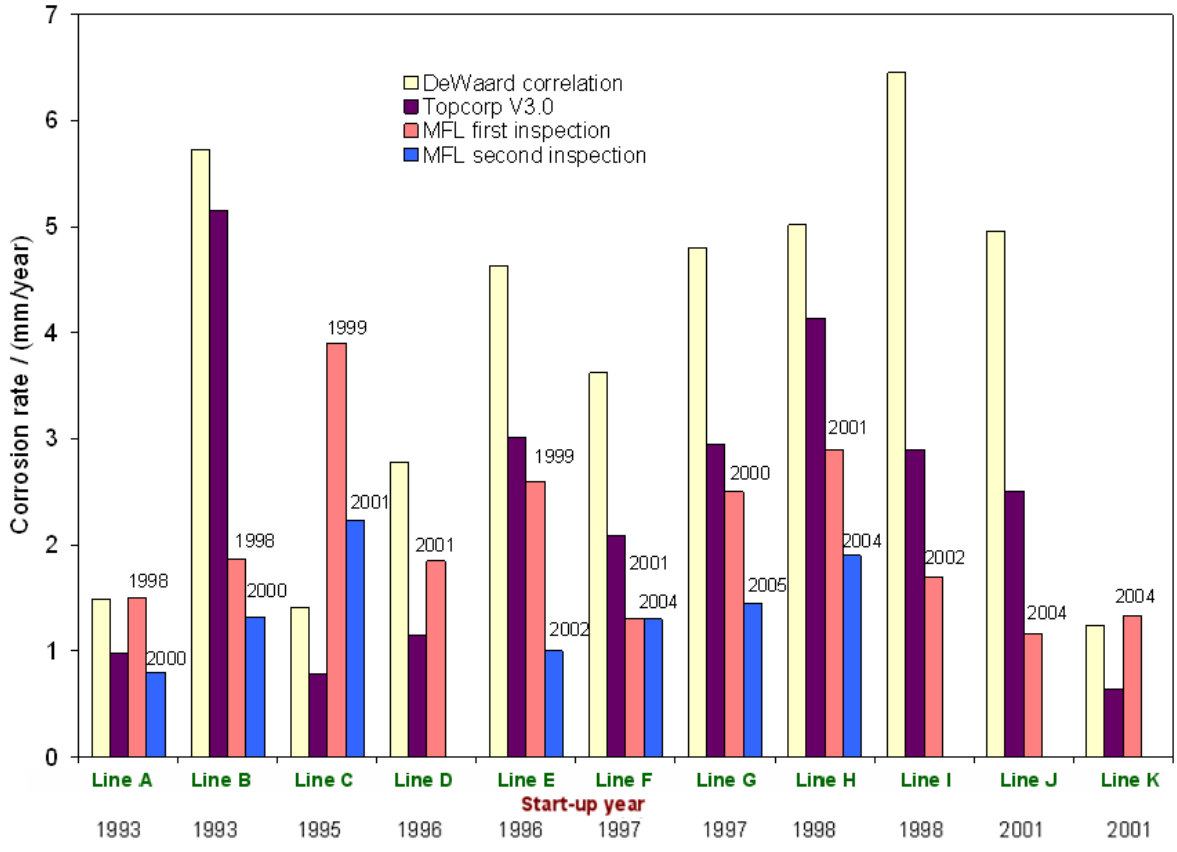

FIGURE 14: Comparison between DeWaard's correlation, selected model prediction and MFL data